Desalination and Water Treatment
www.deswater.com

doi: 10.5004/dwt.2017.20974

96 (2017) 169–177
November

Visible light photocatalytic degradation of methylene blue by $H_2O_2/NiFe_2O_4$ synthesized from wastewater

Dan Chen*, Weide Wang, Fan Zhang, Yan Yang, Guangren Qian

School of Environmental and Chemical Engineering, Shanghai University, No. 99 Shangda Road, Shanghai 200444, China, Tel. +86 2166137784; emails: dchen@shu.edu.cn, chendan_shu@hotmail.com (D. Chen), 714279980@qq.com (W. Wang), zhf2626@sina.com (F. Zhang), 1532436131@qq.com (Y. Yang), grqian@shu.edu.cn (G. Qian)

Received 30 January 2017; Accepted 26 May 2017

ABSTRACT

In this study, a novel magnetic $NiFe_2O_4$ photocatalyst was produced from electroplating wastewater and pickling waste liquor via microwave hydrothermal method. It was shown that 99% of heavy metal ions (Fe^{3+} and Ni^{2+}) in the wastewater could be effectively removed through precipitation. And physicochemical properties of the material were characterized by several techniques, such as X-ray diffraction, scanning electronic microscopy and vibrating sample magnetometer. The values of saturation magnetization of magnetic $NiFe_2O_4$ was about 13.28 emu/g. In addition, photocatalytic degradation of methylene blue (MB) was studied using $NiFe_2O_4$ with H_2O_2 under visible light. The main influence factors (pH, the dosage of $NiFe_2O_4$ and concentration of MB) were investigated, which showed that the maximum MB removal efficiency could reach 99%. Degradation kinetics data followed the pseudo-first-order model. And there was a synergistic effect between $NiFe_2O_4$ and H_2O_2 in the visible light photocatalytic advanced oxidation process. H_2O_2 was activated by $NiFe_2O_4$ and generated hydroxyl radicals (·OH). Meanwhile, the mechanism of the reaction was also discussed in this paper.

Keywords: Heavy metal wastewater; Ferrite; Methylene blue; Hydroxyl radicals; Degradation

1. Introduction

With the development of economy and society, the increasing pollution of heavy metal wastewater has attracted more attention. Typical detrimental properties of heavy metal wastewater include high toxicity, long-term sustainability, mutagenicity and carcinogenicity. Main sources of heavy metal wastewater are electroplating and metal surface treatment industry, metal and plastic coating, electronic industry, petroleum refineries, mining, glass production [1], dyeing, surface treatment industry, etc. [2]. Heavy metal cannot be eliminated by environmental microorganisms; and it is more readily absorbed by organisms and enter the biological food chain, which can cause significant harm to the environment and human health [3], which made the removal of metals from wastewater imperative [4]. Therefore, the treatment of heavy metal wastewater has become the research focus of many environmental experts.

Current heavy metal wastewater treatment methods include chemical precipitation [5], ion exchange [6], adsorption [7], membrane filtration [8], electrochemical treatment [9], etc. But with the development of industrialization and strict environmental policies, most of the traditional or single process methods can no longer meet the technical requirements, therefore, diverse new methods such as photocatalytic method, genetic engineering technology and ferrite method have been developed in recent years. Photocatalysis is a kind of technology to treat wastewater by using the active species such as photogenerated electrons and holes on the surface of photocatalyst [10]. Because of its high efficiency, no secondary pollution and other excellent characteristics,

* Corresponding author.

Presented at the 9th International Conference on Challenges in Environmental Science & Engineering (CESE-2016), 6–10 November 2016, Kaohsiung, Taiwan.

how to choose a more suitable catalyst to further improve the application value in the industry has become a new hot spot in the field of wastewater treatment. Ferrite method is adding iron to the heavy metal wastewater by controlling the process conditions. A variety of metal ions form insoluble ferrite grains in the wastewater, and then by means of solid–liquid separation, the removal of heavy metals was achieved. This method can not only effectively remove almost all kinds of heavy metal ions but also avoid secondary pollution caused by most of the traditional methods. $NiFe_2O_4$ nanoparticles are one of the most useful ferrite due to their characteristics of moderate saturation magnetization [11], strong catalytic property [12], photo-chemical stability [13] and high adsorption capacity [14].

Printing and dyeing wastewater is processed by printing and dyeing factory, which mainly consists of large-volume complex substances that contain many organic compounds with toxicity and poor biodegradability [15]. Because of the difficulty of degradation of dyes, it is difficult to completely degrade them by the traditional single-treatment process. Therefore, the research on the degradation of dyes is mainly focused on the combination of various technologies, such as microwave radiation treatment method, microwave–H_2O_2 combination method, multi-phase UV–ozone oxidation method, electric Fenton and microwave method, etc.

Fenton reaction is considered to be the most promising technology for the treatment of refractory organics in water because it is cost-effective, simple and gives good refractory pollutant degradation [16–19]. Among these techniques, the photo-Fenton process has emerged as a prominent solution to treat chemical contaminants [20], which overcomes the problem of poor efficiency of single Fenton method, improve the wastewater biodegradability and the mineralization of organic matter in dye wastewater. Therefore, the photo-Fenton process has demonstrated a great advantage in the treatment of high-concentration and difficult degradation wastewater [21]. But at present, there are still some limitations in the study of the photo-Fenton method. First of all, Fe^{2+} gets easily inactivated in the photo-Fenton reaction; second, the use of ferric ions results in colored effluents and the formation of iron sludge. In addition, the photo-Fenton reaction works well only under highly acidic conditions (pH range of 2–3), which seriously hinders its application and raises the cost [22,23]. Therefore, how to choose an effective and stable assistant to replace Fe^{2+}, and make the reaction possess excellent degradation effect in the visible light has become the focus of research in this field.

This paper adopted ferrite method to treat several heavy metal wastewater and synthesized wastewater-based $NiFe_2O_4$ with H_2O_2 and visible light to establish a photo-Fenton-like system, the degradation mechanism of dye wastewater by photocatalysis and Fenton reaction is explored. The specific objectives of this project were: (1) study on the effect of treatment of various heavy metal wastewater by ferrite method simultaneously and physicochemical properties of synthesized $NiFe_2O_4$; (2) the influence effects on the degradation by photo-Fenton system were analyzed; (3) the mechanism of degradation of dyes by photo-Fenton-like system was further investigated by means of blank control and the addition of a certain amount of EDTA and tert-butyl alcohol as masking agent.

2. Experimental setup

2.1. Materials

Pickling waste liquor was obtained from Shanghai Second Steel Co., Ltd. (Baoshan District, Shanghai). Electroplating wastewater was provided by the Shanghai Xin Sheng electroplating factory. The concentrations of Fe^{3+} and Ni^{2+} in pickling waste liquor and electroplating wastewater are shown in Table 1. Sodium hydroxide (NaOH), hydrochloric acid (HCl), nitric acid (HNO_3), disodium ethylenediaminetetraacetic acid (EDTA-2Na), hydrogen peroxide (H_2O_2, 30%), sodium nitrite ($NaNO_2$), sodium tetraborate ($Na_2B_4O_7{\cdot}10H_2O$), methylene blue (MB) and absolute alcohol (C_2H_5OH) were purchased from Sinopharm Chemical Reagent Co., Ltd. (Shanghai, China). All chemicals were analytical grade reagents and were used as received without further purification.

2.2. Synthesis of $NiFe_2O_4$

The wastewater-based $NiFe_2O_4$ magnetic material was synthesized by microwave hydrothermal process. In a typical synthesis, the volume ratio of two kinds of wastewater was determined by $n(M^{3+}):n(M^{2+}) = 2:1$ in the mixed solution. 12 g NaOH was dissolved in a certain amount of secondary water at room temperature, then the volume was transferred to a 100 mL volumetric flask after NaOH was completely dissolved. The NaOH solution was added to the mixture by a syringe needle adjusting pH to 13. Then the mixture which has been adjusted for pH was poured into the reaction tank, and the microwave hydrothermal reaction was carried out in the microwave digestion apparatus. The reaction temperature (T) was 180°C, the reaction time (t) was 30 min, and the mixture was cooled to room temperature after the reaction. The solution is cooled uniformly upside down in a centrifuge tube, and centrifuged for three to five times with suction device filtering cracking, dried for 24 h in a vacuum oven at 60°C. The final powder was wastewater-based $NiFe_2O_4$ magnetic material before calcination. Afterwards, the $NiFe_2O_4$ powder was calcinated at 950°C for 6 h to prepare the after calcinations wastewater-based $NiFe_2O_4$ magnetic material.

2.3. Characterization

The powder X-ray diffraction experiment (XRD, Model XD-3A, Shimadzu Co., Japan) with Cu-Kα radiation (λ = 0.154 nm, 34 kV, 20 mA) at the scanning rate of 8°/min

Table 1
The concentration of Fe^{3+} and Ni^{2+} in pickling waste liquor and electroplating wastewater before and after $NiFe_2O_4$ preparation

	Concentration (mg/L)			
	Before treatment		After treatment	
	Fe^{3+}	Ni^{2+}	Fe^{3+}	Ni^{2+}
Pickling waste liquor	54,612	1,955	4	UD
Electroplating wastewater	UD	3,629	UD	UD

Note: UD related to undetected.

from 2θ = 10° to 80° was employed to determine the crystal forms of the samples. Morphological observations were conducted using the scanning electronic microscopy (SEM, Hitachi H-800). The saturation magnetization of the sample was measured by the vibrating sample magnetometer (VSM, 7407 type, Lakeshore Company, USA). XPS measurements (Krato Axis ULTRA, Physical Electronics) was used to explore the variety of Fe and Ni ions before and after photodegradation reaction.

2.4. Adsorption of MB by wastewater-based $NiFe_2O_4$

400 mL MB solution with a concentration of 10–25 mg/L and $NiFe_2O_4$ with a concentration of 0.5–2 g/L were added to 1 L glass beaker at the room temperature in the dark, stirring by the electric machinery of 850 rpm. Then sampled after half an hour (>2.5 mL), followed by centrifugal separation (3,000 rpm, 5 min). The sample was removed to the colorimetric tube and set volume by a 5 mL pipette. Afterwards, the absorbance of the sample was measured by a WFZ UV-4802H spectrophotometer using a 10 mm cuvette at the wavelength of 664 nm and the concentration of MB was calculated.

2.5. Degradation of MB by $NiFe_2O_4/H_2O_2$/visible light system

The influence of initial concentration of MB, pH and the dosage of $NiFe_2O_4$ on the degradation of MB was investigated. Based on section 2.4, 1 mL H_2O_2 solution (30%) was added to above solution with the visible light source, stirring by the electric machinery of 850 rpm to the end of photodegradation. The photodegradation process lasted for 3.5 h, sampled every half an hour and 1 mL H_2O_2 solution (30%) was added every an hour, followed by centrifugal separation (3,000 rpm) for 5 min, then the absorbance of MB was measured by spectrophotometric method and the concentration of residual MB at sampling points was calculated.

The blank experiment: MB solution with a concentration of 20 mg/L was prepared, and the pH was adjusted to 5, then 400 mL MB solution was transferred into a 1 L glass beaker. Photocatalytic and adsorption reaction was carried out without $NiFe_2O_4$.

EDTA-2Na masking controlled experiment: MB solution with a concentration of 20 mg/L was prepared, and the pH was adjusted to around 5, then 400 mL MB solution was transferred into a 1 L glass beaker. 0.4 g $NiFe_2O_4$ and 0.15 g EDTA-2Na were added to adsorption and photocatalytic reaction.

Butanol masking controlled experiment: MB solution with a concentration of 20 mg/L was prepared, and the pH was adjusted to around 5, then 400 mL MB solution was transferred into a 1 L glass beaker. 0.4 g $NiFe_2O_4$ and 0.03 mL tert-butyl alcohol were added to adsorption and photocatalytic reaction.

2.6. Determination of MB dye concentration

0.25, 0.5, 1, 1.5, 2 and 2.5 mL standard solution of MB (20 mg/L) were added to 10 mL colorimetric tube by pipettes, added to 10 mL scale by secondary water. The absorbance of MB was measured at 664 nm with 1 cm glass cuvette by WFZ UV-4802H spectrophotometer. The different water samples were centrifuged, followed by 2.5 mL supernatant of samples were transferred to 10 mL colorimetric tubes, added to 10 mL scale by secondary water.

The concentration of MB in samples can be calculated as follows:

$$A = kC \tag{1}$$

where A was the absorbance of MB in the solution after a certain period, k was the slope of the standard curve and C was the concentration of MB (mg/L) in the sample.

2.7. Calculation of degradation rate of MB

The degradation rate of MB can be expressed as:

$$x = \left(1 - \frac{C}{C_0}\right) \times 100\% \tag{2}$$

where C was the concentration of MB in the solution at a certain time (mg/L), C_0 was the initial concentration of MB (mg/L).

3. Results and discussion

3.1. Characterization of samples

The XRD patterns of wastewater-based $NiFe_2O_4$ before calcination was shown in Fig. 1(a). The diffraction peaks at 18.4°, 30.3°, 35.7°, 37.3°, 43.3°, 53.8°, 57.3°, 63.0° and 74.5° were matching well with the (111), (220), (311), (222), (400), (422), (511), (440) and (533) crystalline planes of $NiFe_2O_4$, respectively. In contrast, $NiFe_2O_4$ with much stronger diffraction peaks and better crystal structure could be observed after calcination, as shown in Fig. 1(b).

The morphology of as-synthetic $NiFe_2O_4$ before and after calcination were observed by SEM. $NiFe_2O_4$ appeared bulk-like in Fig. 2(a), cluster size with diameter approximately 1.5 μm can be observed. In comparison, a more homogeneous distribution was presented after calcination in Fig. 2(b). Average cluster size was approximately 0.15 μm. Regulated crystallinity was demonstrated after calcination.

The magnetic hysteresis loops were depicted in Fig. 3. The prepared wastewater-based $NiFe_2O_4$ without coercivity and remanence showed typical superparamagnetism, it exhibited a typical ferromagnetic behavior at room temperature and the saturation magnetization was 13.28 emu/g. Providing the possibility for the recovery of magnetic ferrite.

3.2. Adsorption of MB by wastewater-based $NiFe_2O_4$

In order to study the adsorption properties of the wastewater-based $NiFe_2O_4$, the adsorption reaction was set up in the dark for 0.5 h under different experiment conditions of pH, $NiFe_2O_4$ dosage and initial concentration of MB. The adsorption properties of MB by $NiFe_2O_4$ characterized in the dark for 0.5 h were presented in Fig. 4. As can be seen from the graph, the adsorption rate of MB by $NiFe_2O_4$ increased with the decrease of pH and initial concentration of MB, and the increase of $NiFe_2O_4$ dosage. However, in general,

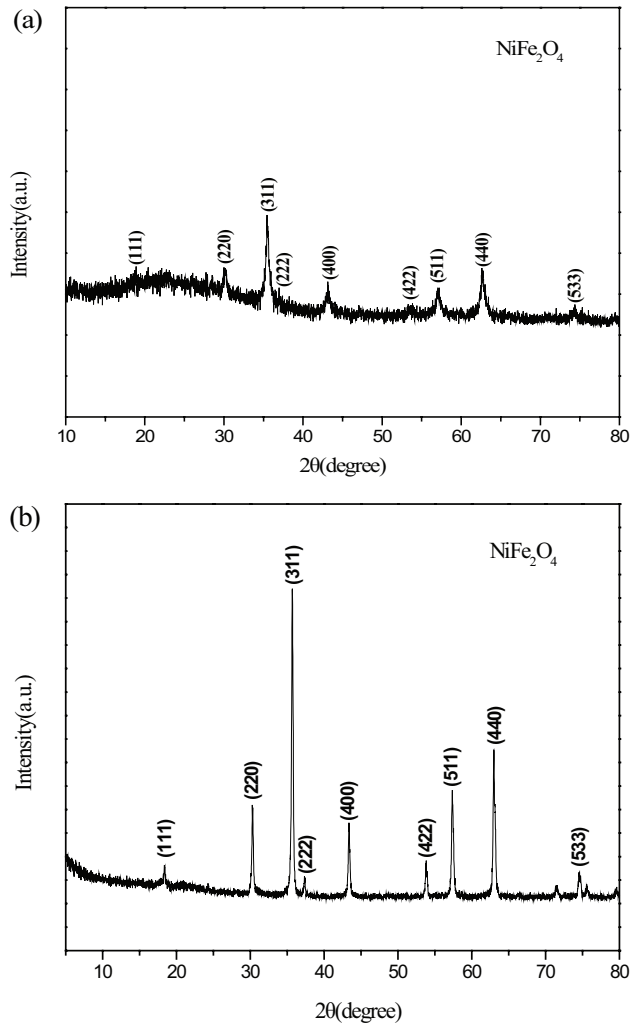

Fig. 1. X-ray diffraction patterns of wastewater-based $NiFe_2O_4$ before calcination (a) and after calcination (b).

the maximum adsorption rate of MB is not more than 15% under different conditions. Therefore, the adsorption performance of wastewater-based $NiFe_2O_4$ is not suitable to be used as a good adsorbent.

3.3. Degradation of MB by $NiFe_2O_4/H_2O_2$/visible light system

The comparison of the degradation effect of MB by H_2O_2/visible light system and $NiFe_2O_4/H_2O_2$/visible light system is shown in Fig. 5. After 3.5 h, the degradation rate of MB by H_2O_2/visible light system was only 40%, while the degradation rate of MB by $NiFe_2O_4/H_2O_2$/visible light system could reach more than 90%. The main reason is that H_2O_2/visible light system can only use a small amount of ·OH produced from H_2O_2 to oxidize MB, however, in the $NiFe_2O_4/H_2O_2$/visible light system, hole produced from $NiFe_2O_4$ under visible light can oxidize H_2O_2 in solution, so that produce more ·OH to oxidize more MB [24]. Therefore, we can conclude that the presence of $NiFe_2O_4$ can significantly improve the degradation effect of MB by $NiFe_2O_4/H_2O_2$/visible light.

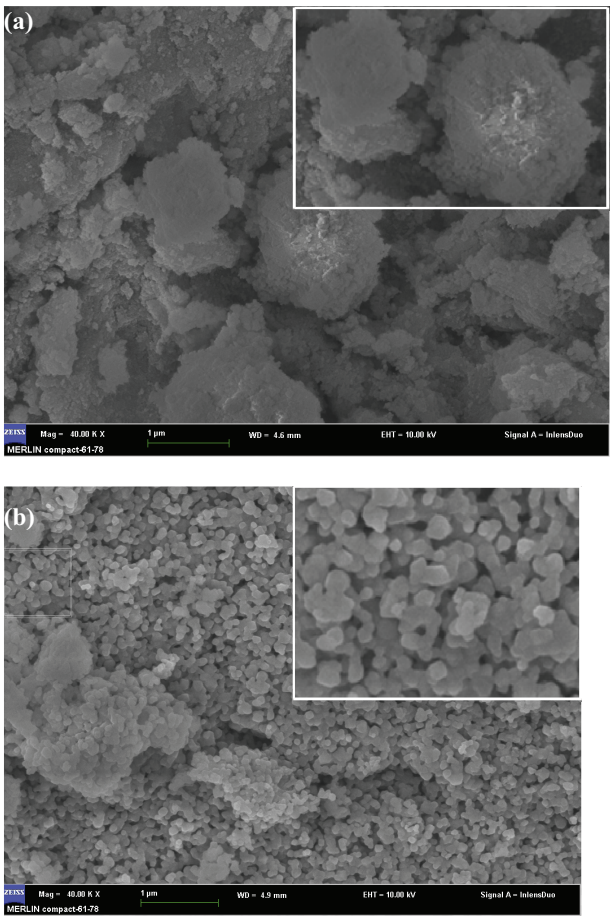

Fig. 2. The SEM images of $NiFe_2O_4$ before calcination (a) and after calcination (b).

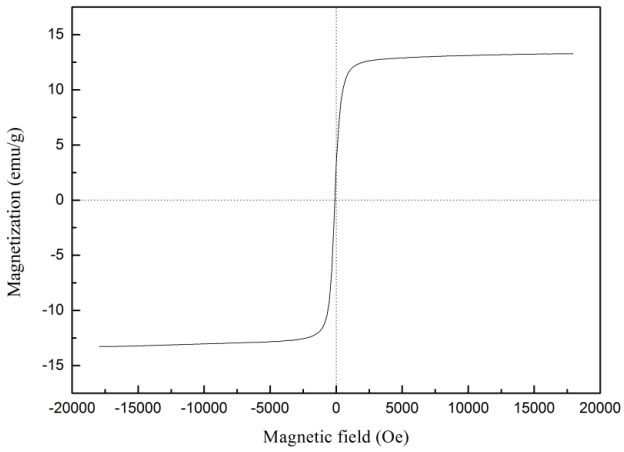

Fig. 3. Room temperature magnetic hysteresis loops for $NiFe_2O_4$.

3.3.1. Degradation of MB under different pH

Degradation effect of MB by $NiFe_2O_4$ combined with H_2O_2 and visible light under different pH was shown in Fig. 6. The opening 0.5 h was dark adsorption experiments, 0.5 h was the beginning of the photodegradation reaction. The reaction conditions of photodegradation experiment were as follows:

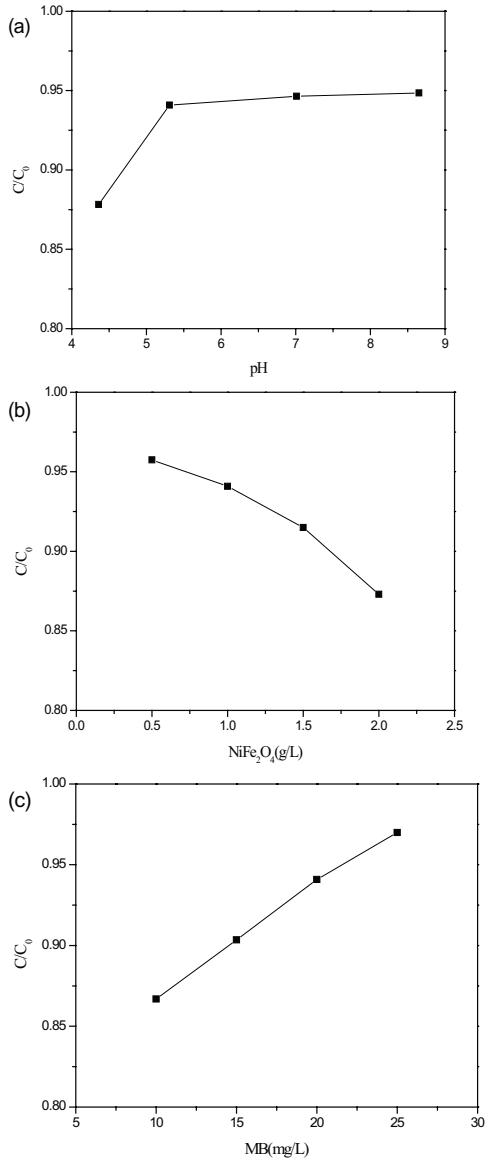

Fig. 4. The adsorption properties of MB by $NiFe_2O_4$ under different conditions: pH (a), $NiFe_2O_4$ dosage (b) and initial concentration of MB (c).

the initial concentration of MB was 20 mg/L, the addition of 30% H_2O_2 was 1 mL/h after the photocatalytic reaction begins, the dosage of $NiFe_2O_4$ was 1 g/L and the pH values were 4, 5, 7 and 8, respectively.

The content change of MB with time under different pH in the $NiFe_2O_4/H_2O_2$/visible light system was shown in Fig. 6(a), the kinetic equation fitting curve of MB degradation was shown in Fig. 6(b). Under the different conditions of pH, all reaction showed a certain degradation effect. Obviously, the photo-Fenton-like system at pH 4 and 5 had the MB decomposition efficiency for 95%. When the solution becomes neutral or alkaline, the degradation rate decreased significantly. As the pH was 7, degradation rate can only reach less than 50%.

The degradation of MB conforms to the first-order kinetic model, where C and C_0 are the concentration of MB at

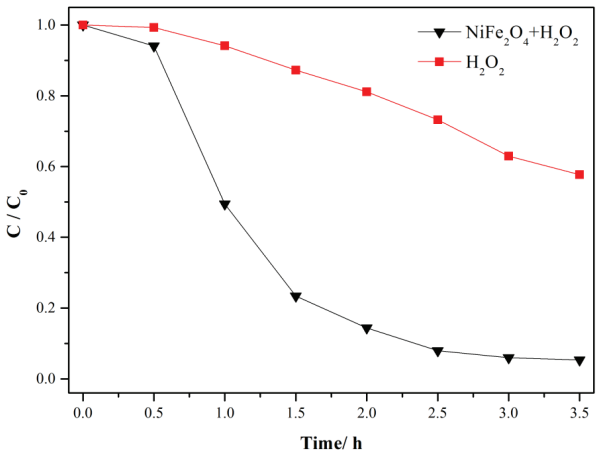

Fig. 5. Degradation of MB by $NiFe_2O_4/H_2O_2$/visible light system.

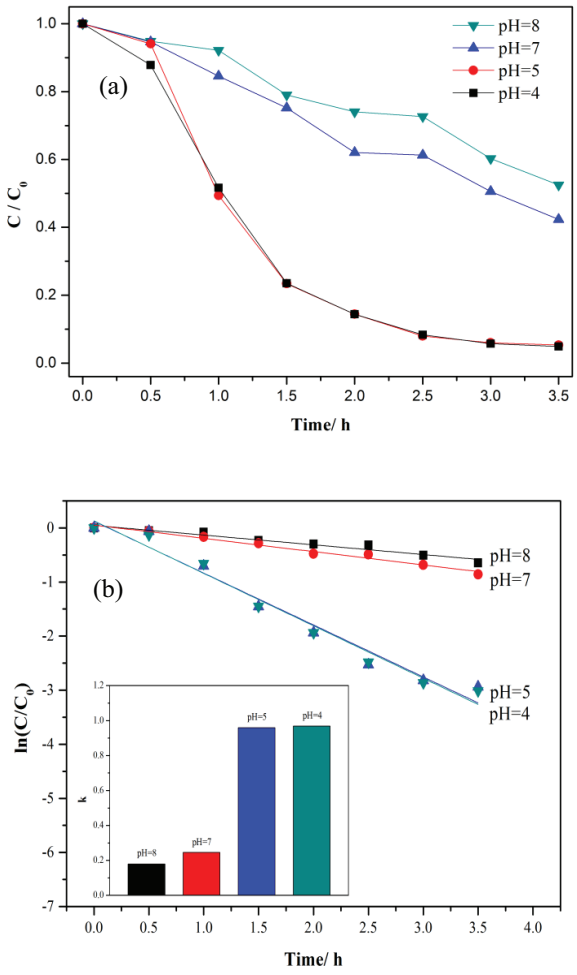

Fig. 6. (a) Degradation effect of MB. (b) The kinetic equation fitting curve of MB degradation under different pH conditions by $NiFe_2O_4/H_2O_2$/visible light system.

time t and time t = 0, respectively, and the degradation rate constant is k. We can see from Fig. 6(a) that the reaction system almost simultaneously reached the maximum decomposition

efficiency when pH = 4 and 5, this is because when the pH is about 3~5, the main form of ferric ions is $[Fe(OH)]^{2+}$, the hydroxyl complex has excellent light and energy absorption, which can not only absorb light to generate more ·OH but also strengthen the reduction of Fe^{3+}, thus it can promote the decomposition of H_2O_2, which accelerate the reaction rate remarkably. The reaction equation can be described as follows [24]:

$$[Fe(OH)]^{2+} + h\upsilon \rightarrow Fe^{2+} + \cdot OH \quad (3)$$

$$Fe^{2+} + H_2O_2 \rightarrow Fe^{3+} + \cdot OH + OH^- \quad (4)$$

$$Fe^{3+} + H_2O_2 \rightarrow [Fe(HO_2)]^{2+} + H^+ \quad (5)$$

$$[Fe(HO_2)]^{2+} \rightarrow Fe^{2+} + \cdot HO_2 \quad (6)$$

Obviously, both degradation effect and degradation rate are almost same when pH is 4 and 5. In order to save the amount of buffer solution, pH of following experiments is set to 5.

3.3.2. Degradation of MB under different $NiFe_2O_4$ dosage

Degradation effect of MB by $NiFe_2O_4$ combined with H_2O_2 and visible light with different $NiFe_2O_4$ dosage is shown in Fig. 7. The opening 0.5 h is dark adsorption experiments, 0.5 h is the beginning of the photodegradation reaction. The reaction conditions of photodegradation experiment are as follows: the initial concentration of MB was 20 mg/L, the reaction pH was approximately 5, the addition of 30% H_2O_2 was 1 mL/h and the dosage of $NiFe_2O_4$ was 0, 0.5, 1, 1.5 and 2 g/L, respectively.

The content change of MB with time under different $NiFe_2O_4$ dosage in the $NiFe_2O_4/H_2O_2$/visible light system is shown in Fig. 7(a), the kinetic equation fitting curve of MB degradation is shown in Fig. 7(b). Obviously, there is only H_2O_2 and visible light without $NiFe_2O_4$ in the reaction solution, the degradation rate of MB is only about 40%. First, the Fenton-like system cannot form due to lack of iron ions; second, it becomes H_2O_2/visible light system because of lack of photocatalyst $NiFe_2O_4$. Therefore, it can be seen that H_2O_2/visible light system can be inefficient and not applicable. Comprehensive above chart shows that when adding a small amount of $NiFe_2O_4$ (0.5 g/L), the degradation rate of MB was two times more than without $NiFe_2O_4$. The degradation rate of MB increased linearly with the increase of the amount of $NiFe_2O_4$. When the dosage of $NiFe_2O_4$ was increased to 2.0 g/L, the degradation rate of MB reached more than 90% in 0.5 h, at the end of the reaction reached more than 99% (99.3%), and the sample completely faded in visible light, achieving decolorization and degradation double requirements completely at low-energy conditions with a small amount of H_2O_2.

3.3.3. Degradation of MB under different MB initial concentration

Degradation effect of MB by $NiFe_2O_4$ combined with H_2O_2 and visible light with different MB initial concentration is shown in Fig. 8. The opening 0.5 h is dark adsorption experiment, 0.5 h is the beginning of the photodegradation

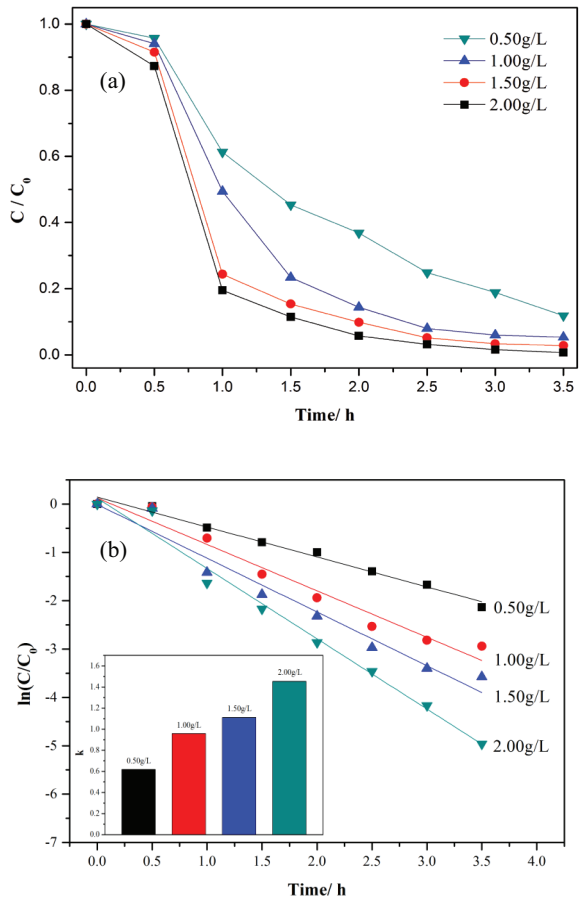

Fig. 7. (a) Degradation effect of MB. (b) The kinetic equation fitting curve of MB degradation under different $NiFe_2O_4$ dosage conditions by $NiFe_2O_4/H_2O_2$/visible light system.

reaction. The reaction conditions of photodegradation experiment are as follows: the amount of $NiFe_2O_4$ is 2.0 g/L, the reaction pH is approximately 5, the addition of 30% H_2O_2 is 1 mL/h, the dosage of $NiFe_2O_4$ is 1 g/L and the initial concentrations of MB are 10, 15, 20 and 25 mg/L.

The degradation rate of MB under different initial concentration of MB is given in Fig. 8(a) and the kinetic equation fitting curve of MB degradation is given in Fig. 8(b), we can see that the degradation rate of MB decreased linearly with the increase of the initial concentration of MB. Among them, when the initial concentration of MB was 10 mg/L, the degradation rate of MB can reach more than 98% after 3 h, but when the concentration of MB was 25 mg/L, degradation rate decreased to 89.7% and the reaction rate is reduced by about 50%, hence light-assisted Fenton-like system application in the treatment of high-concentration wastewater is not advisable, however, which can achieve ideal effect in the treatment of low-concentration wastewater.

3.4. Degradation mechanism of MB by $NiFe_2O_4/H_2O_2$/visible light system

Degradation mechanism of MB by the $NiFe_2O_4/H_2O_2$/visible light system is shown in Fig. 9. The opening 0.5 h is dark adsorption experiments, 0.5 h is the beginning of the

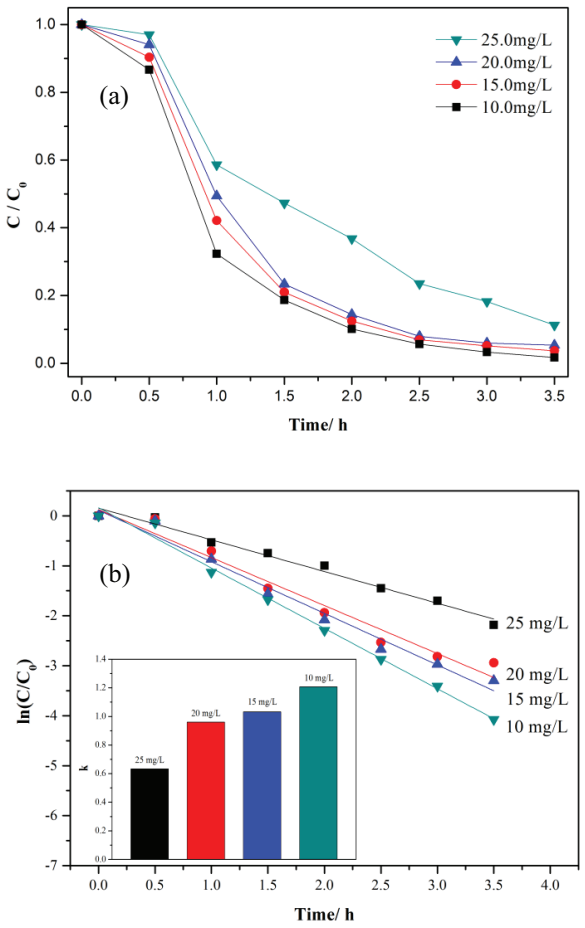

Fig. 8. (a) Degradation effect of MB. (b) The kinetic equation fitting curve of MB degradation with different MB concentrations by $NiFe_2O_4/H_2O_2$/visible light system.

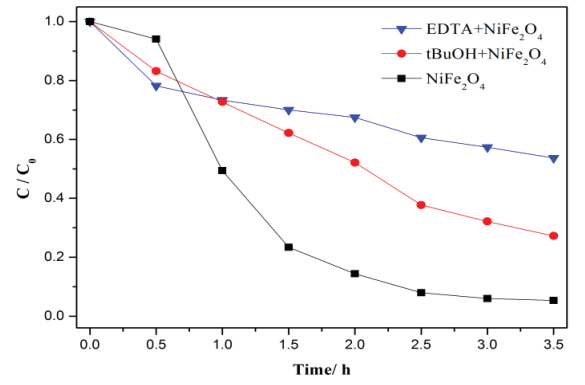

Fig. 9. Degradation effect of MB by $NiFe_2O_4$ in the control experiment.

photodegradation reaction. The reaction conditions of photodegradation experiment are as follows: initial concentration of MB is 20 mg/L, the reaction pH is approximately 5, the addition rate of H_2O_2 (30%) is 1 mL/h. One group was added to $NiFe_2O_4$, the other two groups were added to $NiFe_2O_4$ (1 g/L) and appropriate amounts of EDTA-2Na and tert-butyl alcohol.

Obviously, in the EDTA-2Na masking controlled experiment, EDTA-2Na plays a role in capture masking on the hole, so the number of ·OH produced by the reaction between hole and electron acceptor decrease, namely the effect of the photocatalyst in photodegradation reaction is shielded to a certain extent. On the contrary, in the control experiment of $NiFe_2O_4$, hole produced from $NiFe_2O_4$ under visible light can produce more ·OH to oxidize more MB in solution. In terms of reaction rate, the EDTA-2Na masking controlled experiment have remarkable difference with the control experiment of $NiFe_2O_4$, thereby, it indicated that the main function of photodegradation process in this system is $NiFe_2O_4$ and Fenton-like reaction in the $NiFe_2O_4/H_2O_2$/visible light system does not play a leading role, so we can conclude that cubic spinel type ferrite is an excellent photocatalyst [25]. This is also reflected in the results of the inhibition of ·OH generation in tert-butyl alcohol. Moreover, it can also be observed while the degradation rate of MB in tert-butanol system compared with original system is only 20%, but the reaction rate is reduced to less than 40%, which shows that there is a problem of low reaction rate in pure photodegradation. Therefore, it is necessary to establish photo-Fenton-like system.

Fig. 10 shows the XPS spectra of (a) Ni2p and (b) Fe2p on the $NiFe_2O_4$ catalyst (1) before the photodegradation reaction and (2) after the photodegradation reaction. As shown in Fig. 10(a), the main peak of $Ni2p_{3/2}$ at approximately 855 eV and the $Ni2p_{1/2}$ peak at approximately 874 eV were observed without a slight shift to higher energy after the visible light photocatalytic degradation reaction [26,27]. These peaks indicate the unimportant catalytic role of Ni. The XPS peaks of $Fe2p_{3/2}$ and $Fe2p_{1/2}$ are shown in Fig. 10(b). Of the two peaks, $Fe2p_{3/2}$ peak is narrower and stronger than $Fe2p_{1/2}$. $Fe2p_{3/2}$ signals and $Fe2p_{1/2}$ signals are 711 eV and 724 eV, respectively. The $Fe2p_{3/2}$ peak at approximately 711 eV and the $Fe2p_{1/2}$ peak at approximately 724 eV appeared significant change after irradiation. This result suggests noticeable differences in the chemical environments or states of Fe before and after the photo-Fenton process [28,29].

4. Conclusion

In this paper, pickling waste liquor from Shanghai Second Steel Co., Ltd. and electroplating wastewater from Shanghai Xin Sheng electroplating factory are used to fabricate wastewater-based $NiFe_2O_4$ by microwave hydrothermal method. The treatment effect of heavy metal wastewater is analyzed. At the same time, MB is selected as the target pollutants, the effect of heavy metal wastewater degradation of the pollutants by the $NiFe_2O_4/H_2O_2$/visible light system was investigated, and the effects of pH, $NiFe_2O_4$ dosage and initial concentration of MB on the degradation were investigated by the variable-controlling approach. Finally, a series of controlled experiments were carried out to discuss the reaction mechanism of the $NiFe_2O_4/H_2O_2$/visible light system.

The main conclusions of this paper are as follows: (1) Synthesis of magnetic wastewater-based $NiFe_2O_4$ by microwave hydrothermal method. The removal rate of Fe and Ni in the pickling waste liquor and electroplating wastewater reached above 99%, and the heavy metal content reached

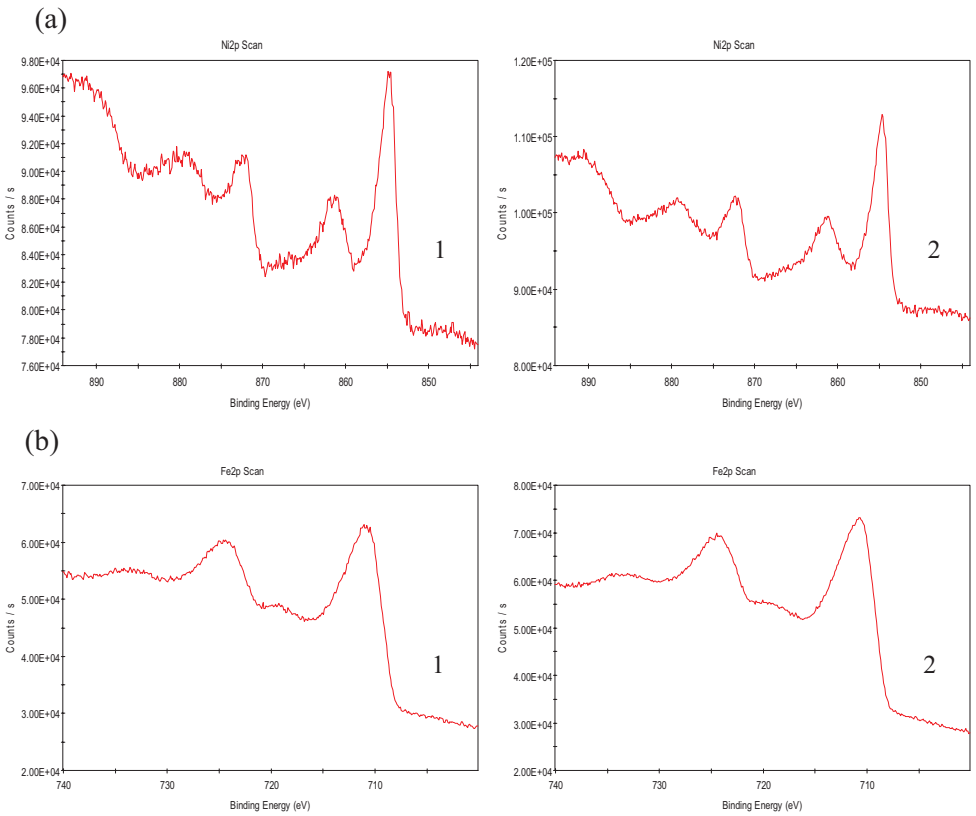

Fig. 10. XPS spectra of (a) Ni2p and (b) Fe2p on the $NiFe_2O_4$ catalyst (1) before the photodegradation reaction and (2) after the photodegradation reaction.

the discharge standard; (2) XRD, SEM and VSM were used to analyze the hydrothermal synthesis of wastewater-based $NiFe_2O_4$ as a cubic spinel structure, which showed a typical superparamagnetic, and the saturation magnetization of $NiFe_2O_4$ was 13.28 emu/g; (3) The adsorption capacity of MB by $NiFe_2O_4$ was poor, and the maximum adsorption capacity was only 2.43 mg/g; (4) In terms of $NiFe_2O_4/H_2O_2$/visible light system, the degradation of MB was in accord with the first-order kinetic model. The increase of $NiFe_2O_4$ dosage, the decrease of pH and the decrease of the initial concentration of MB could accelerate the degradation of MB in a certain range; (5) In the $NiFe_2O_4/H_2O_2$/visible light system, photocatalytic degradation reaction plays a leading role while photo-Fenton-like reaction plays a supporting role which can accelerate the reaction rate significantly.

Acknowledgments

This work was supported by National Nature Science Foundation of China (Nos. 51274138, 50974086 and 50704023), the Innovation Program of Shanghai Municipal Education Commission (14YZ014) and the Program for Innovative Research Team in University (No. IRT13078).

References

[1] M.E. Argun, S. Dursun, C. Ozdemir, M. Karatas, Heavy metal adsorption by modified oak sawdust: thermodynamics and kinetics, J. Hazard. Mater., 141 (2007) 77–85.

[2] K. Vijayaraghavan, J. Jegan, K. Palanivelu, M. Velan, Batch and column removal of copper from aqueous solution using a brown marine alga *Turbinaria ornata*, Chem. Eng. J., 106 (2005) 177–184.

[3] N. Hafiza, A. Razak, S.M. Praveena, Z. Hashim, A. Zaharin, Drinking water studies: a review on heavy metal, application of biomarker and health risk assessment, J. Epidemiol. Global Health, 5 (2015) 297–310.

[4] F. Wang, X.W. Lu, X.Y. Li, Selective removals of heavy metals (Pb^{2+}, Cu^{2+}, and Cd^{2+}) from wastewater by gelation with alginate for effective metal recovery, J. Hazard. Mater., 308 (2016) 75–83.

[5] M.T. Alvarez, C. Crespo, B. Mattiasson, Precipitation of Zn(II), Cu(II) and Pb(II) at bench-scale using biogenic hydrogen sulfide from the utilization of volatile fatty acids, Chemosphere, 66 (2007) 1677–1683.

[6] T.M. Zewail, N.S. Yousef, Kinetic study of heavy metal ions removal by ion exchange in batch conical air spouted bed, Alexandria Eng. J., 54 (2015) 83–90.

[7] A.A. Ismail, R.M. Mohamed, I. AIbrahim, G. Kini, B. Koopman, Synthesis, optimization and characterization of zeolite A and its ion exchange properties, Colloids Surf. A, 366 (2010) 80–87.

[8] S.K. Gunatilake, Methods of removing heavy metals from industrial wastewater, J. Multidiscip. Eng. Sci. Stud., 1 (2015) 12–18.

[9] X. Chen, G. Huang, J. Wang, Electrochemical reduction/oxidation in the treatment of heavy metal wastewater, J. Metall. Eng., 2 (2013) 161–164.

[10] E. Friehs, Y. AlSalka, R. Jonczyk, A. Lavrentieva, A. Jochums, J.-G. Walter, F. Stahl, T. Scheper, D. Bahnemann, Toxicity, phototoxicity and biocidal activity of nanoparticles employed in photocatalysis, J. Photochem. Photobiol. C, 29 (2016) 1–28.

[11] A. Ren, C. Liu, Y. Hong, W. Shi, S. Lin, P. Li, Enhanced visible-light-driven photocatalytic activity for antibiotic degradation using magnetic $NiFe_2O_4/Bi_2O_3$ heterostructures, Chem. Eng. J., 258 (2014) 301–308.

[12] H.Y. Zhu, R. Jiang, S.H. Huang, J. Yao, F.Q. Fu, J.B. Li, Novel magnetic $NiFe_2O_4$/ multi-walled carbon nanotubes hybrids: facile synthesis, characterization, and application to the treatment of dyeing wastewater, Ceram. Int., 41 (2015) 11625–11631.
[13] T. Peng, X. Zhang, H. Lv, L. Zan, Preparation of $NiFe_2O_4$ nanoparticles and its visible-light-driven photoactivity for hydrogen production, Catal. Commun., 28 (2012) 116–119.
[14] S.V. Bhosale, N.S. Kanhe, S.V. Bhoraskar, S.K. Bhat, R.N. Bulakhe, J.J. Shim, V.L. Mathe, Micro-structural analysis of $NiFe_2O_4$ nanoparticles synthesized by thermal plasma route and its suitability for BSA adsorption, J. Mater. Sci., 26 (2015) 216–230.
[15] Q. Chen, Y. Zhang, D. Zhang, Y. Yang, Ag and N co-doped TiO_2 nanostructured photocatalyst for printing and dyeing wastewater, J. Water Process Eng., 16 (2017) 14–20.
[16] Y. Deng, J.D. Englehardt, Treatment of landfill leachate by the Fenton process, Water Res., 40 (2006) 3683–3694.
[17] A.Z. Gotvajn, J. Zagorc-Koncan, M. Cotman, Fenton's oxidative treatment of municipal landfill leachate as an alternative to biological process, Desalination, 275 (2011) 269–275.
[18] E. Kattel, M. Trapido, N. Dulova, Treatment of landfill leachate by continuously reused ferric oxyhydroxide sludge-activated hydrogen peroxide, Chem. Eng. J., 304 (2016) 646–654.
[19] S. Cortez, P. Teixeira, R. Oliveira, M. Mota, Evaluation of Fenton and ozone-based advanced oxidation processes as mature landfill leachate pre-treatments, J. Environ. Manage., 92 (2011) 749–755.
[20] S. Malato, P. Fernández-Ibánez, M.I. Maldonado, J. Blanco, W. Gernjak, Decontamination and disinfection of water by solar photocatalysis: recent overview and trends, Catal. Today, 147 (2009) 1–59.
[21] J.-A. Park, H.-L. Nam, J.-W. Choi, J. Ha, S.-H. Lee, Oxidation of geosmin and 2-methylisoborneol by the photo-Fenton process: kinetics, degradation intermediates, and the removal of microcystin-LR and trihalomethane from Nak-Dong River water, South Korea, Chem. Eng. J., 313 (2017) 345–354.
[22] Z. Ai, L. Lu, J. Li, L. Zhang, J. Qiu, M. Wu, $Fe@Fe_2O_3$ core-shell nanowires as iron reagent. 2. An efficient and reusable sono-fenton system working at neutral pH, J. Phys. Chem. C, 111 (2007) 7430–7436.
[23] J. Yu, X. Yu, B. Huang, X. Zhang, Y. Dai, Hydrothermal synthesis and visible-light photocatalytic activity of novel cage-like ferric oxide hollow spheres, Cryst. Growth Des., 9 (2009) 1474–1480.
[24] N. Chen, G. Fang, D. Zhou, J. Gao, Effects of clay minerals on diethyl phthalate degradation in Fenton reactions, Chemosphere, 165 (2016) 52–58.
[25] K. Tezuka, M. Kogure, Y.J. Shan, Photocatalytic degradation of acetic acid on spinel ferrites MFe_2O_4 (M = Mg, Zn, and Cd), Catal. Commun., 48 (2014) 11–14.
[26] H.W. Nesbitt, D. Legrand, G.M. Bancroft, Interpretation of Ni2p XPS spectra of Ni conductors and Ni insulators, Phys. Chem. Miner., 27 (2000) 357–366.
[27] D. Chen, F. Zhang, Q. Li, W. Wang, G. Qian, Y. Jin, Z. Xu, A promising synergistic effect of nickel ferrite loaded on the layered double hydroxide-derived carrier for enhanced photocatalytic hydrogen evolution, Int. J. Hydrogen Energy, 42 (2017) 867–875.
[28] S.-Q. Liu, B. Xiao, L.-R. Feng, S.-S. Zhou, Z.-G. Chen, C.-B. Liu, F. Chen, Z.-Y. Wu, N. Xu, W.-C. Oh, Z.-D. Meng, Graphene oxide enhances the Fenton-like photocatalytic activity of nickel ferrite for degradation of dyes under visible light irradiation, Carbon, 64 (2013) 197–206.
[29] T. Yamashita, P. Hayes, Analysis of XPS spectra of Fe^{2+} and Fe^{3+} ions oxide materials, Appl. Surf. Sci., 254 (2008) 2441–2449.